Acta Oto-Laryngologica, 2012; Early Online, 1–6

informa
healthcare

ORIGINAL ARTICLE

Superparamagnetic iron oxide-enhanced interstitial magnetic resonance lymphography to detect a sentinel lymph node in tongue cancer patients

DAISUKE MIZOKAMI[1], SHIGERU KOSUDA[2], MASAYUKI TOMIFUJI[1], KOJI ARAKI[1], TAKU YAMASHITA[1], HIROSHI SHINMOTO[2] & AKIHIRO SHIOTANI[1]

[1]*Department of Otolaryngology and* [2]*Department of Radiology, National Defense Medical College, Tokorozawa, Saitama, Japan*

Abstract

Conclusion: This is the first report on human sentinel node (SN) detection by interstitial magnetic resonance (MR) lymphography with superparamagnetic iron oxide (SPIO) in tongue cancer patients who also underwent lymphoscintigraphy. Our results indicate that further studies are warranted, as this novel method may replace current scintigraphic techniques. *Objectives:* To examine the feasibility of interstitial MR lymphography using SPIO for SN detection in the head and neck region. *Methods:* MR images were acquired sequentially at 10 min, 30 min, and 24 h after submucosally injecting 0.1 ml SPIO (ferucarbotran) around the tumor in three patients with tongue cancer without cervical lymph node metastasis (clinical T2N0M0). *Results:* The SNs were clearly visualized in the 10 min interstitial MR lymphography images and were completely concordant with those visualized by ^{99m}Tc-radiocolloid lymphoscintigraphy and a gamma probe in all cases. Iron incorporation into the SNs was confirmed by pathological examination.

Keywords: *Sentinel node navigation surgery, head and neck cancer, lymphoscintigraphy*

Introduction

There have been several reports on the application of sentinel lymph node biopsy (SNB) using ^{99m}Tc-radiocolloid for the management of head and neck cancer patients [1–4]. This technique allows head and neck surgeons to avoid unnecessary neck dissection and reduces the incidence of associated postoperative morbidities, such as shoulder pain and facial edema. However, sentinel node (SN) detection using ^{99m}Tc-radiocolloid has some drawbacks, such as the strict legal regulations governing the use of ^{99m}Tc-radiocolloids that exist in Japan. Moreover, the shine-through phenomenon encountered during the use of these compounds generally hampers SN detection, especially when the SN is located near the ^{99m}Tc-radiocolloid injection site. In addition, an expensive gamma probe is necessary for intraoperative detection of SNs.

Superparamagnetic iron oxides (SPIOs) are nanoparticles that are incorporated into macrophages and other phagocytic cells and have been used as macrophage-imaging agents [5,6]. SPIOs generate a strong negative contrast in gradient echo sequences of magnetic resonance (MR) images. Recently, researchers reported that interstitial MR lymphography with SPIO particles produced excellent results in the detection of SNs, and is already in use for human breast or lung cancer patients [7,8]. Interstitial MR lymphography with SPIO for SN detection in swine tongues has also been reported [9]. We have also reported that interstitial MR lymphography with SPIO was useful in detecting SNs in the head and neck region using a mouse model [10]. However, there are no reports of the clinical use of interstitial MR lymphography with SPIO for SN detection in human head and neck cancer patients.

Correspondence: Akihiro Shiotani MD, Department of Otolaryngology, National Defense Medical College, 3-2 Namiki Tokorozawa Saitama, 359-8513, Japan. Fax: +81 429 96 5212. E-mail: ashiotan@ndmc.ac.jp

(Received 31 August 2012; accepted 20 October 2012)

ISSN 0001-6489 print/ISSN 1651-2251 online © 2012 Informa Healthcare
DOI: 10.3109/00016489.2012.744143

The purpose of the present study was to evaluate the feasibility of interstitial MR lymphography using SPIO for SN detection in human tongue cancer patients and to conduct a comparative study of this technique with the conventional ^{99m}Tc-radiocolloid lymphoscintigraphy.

Material and methods

All procedures used in this study were approved by the Institutional Review Board of the National Defense Medical College and adhered to the institutional guidelines.

Patients

Three tongue cancer patients, without cervical lymph node metastasis (clinical T2N0M0), were enrolled in this study at the National Defense Medical College Hospital between January and May 2012. Informed consent was obtained from the three patients and was documented. None of the patients received preoperative chemotherapy or radiotherapy. All cases were pathologically diagnosed with tongue cancer having squamous cell carcinoma. Neither conventional MR imaging nor ^{18}F-fluorodeoxyglucose (18F-FDG) positron emission tomography/computed tomography (PET/CT) revealed any metastases. Partial laser resection of the tongue and prophylactic supraomohyoid neck dissection (level I–III on the affected side) were planned as the initial treatment in all three individuals.

Interstitial MR lymphography

Interstitial MR lymphography with SPIO was performed 7 days before the surgery. A total of 0.1–0.3 ml ferucarbotran (Resovist^{TM}; Bayer Schering Pharma, Berlin, Germany) was administered submucosally into four sites around each tongue tumor, using a 29 Ga needle and a 0.5 ml syringe (2.78–8.37 mg iron of ferucarbotran). The dose and volume to be injected were determined in accordance with results obtained from previous animal studies [10]. Axial and coronal T1- and T2*-weighted MR images of fast-field echo (FFE) sequences were acquired sequentially at 10 min, 30 min, and 24 h after the submucosal ferucarbotran injection, using a 3 Tesla MR imaging system (Achieva; Philips Medical Systems, Best, The Netherlands).

Lymphoscintigraphy

On the day before the surgery, 1 ml of ^{99m}Tc-phytate (2 mCi, 74 MBq/mL; Fujifilm RI Pharma, Tokyo, Japan) was injected submucosally, using a 27 Ga needle, into four sites around the tumor of the tongue. Immediate rinsing, thereafter, with a mouthwash prevented pooling and swallowing of residual radioactivity. A planar lymphoscintigraphic image was taken 1 h after the injection to detect SNs. Lymphoscintigrams were acquired from at least two different viewpoints with a conventional gamma camera (GCA7200A/DI, Toshiba, Tokyo, Japan). Single photon emission computed tomography (SPECT)/computed tomography (CT) (Symbia T; Siemens AG, Munich, Germany) image data were acquired 15 min after the planar image acquisition in patient 2.

Surgery

Partial glossectomy was initially performed to avoid radiation scatter from the primary tumor. Before SNB, the locations of radioactive lymph nodes were detected using a hand-held gamma probe (Gamma Positioning System; RMD Instruments, Watertown, MA, USA) and marked on the patient's skin. A gamma probe identified SNs during SN biopsy. The amount of radioactivity in excised SNs was scored using a gamma probe and SNs were labeled according to their radioactive and anatomic neck levels [11].

The prophylactic supraomohyoid neck dissection (levels I, II, and III) on the affected side was performed as scheduled, regardless of the results of the SNB.

Histopathologic evaluation of the lymph nodes

Histopathologic evaluation was performed on the SNs and all other dissected lymph nodes. The SNs were rapidly frozen and examined in multiple, 2 mm interval sections after staining with hematoxylin and eosin (H&E) for intraoperative diagnosis. The remaining resected lymph nodes were embedded in paraffin and examined postoperatively, in a single representative cross-section, after H&E staining. The SNs were re-evaluated again as permanent 4 μm thick specimens, at 2 mm intervals, after H&E staining and immunohistochemical staining of cytokeratin. To confirm the presence of iron nanoparticles derived from the injected SPIO, Berlin blue staining of the resected SN specimens was also performed.

Results

SNs were clearly visualized on fast-field echo (FFE) T1- and T2*-weighted MR images at 10 min, 30 min, and 24 h after the injection. Contrast effects, resulting from the presence of ferucarbotran, were detected at

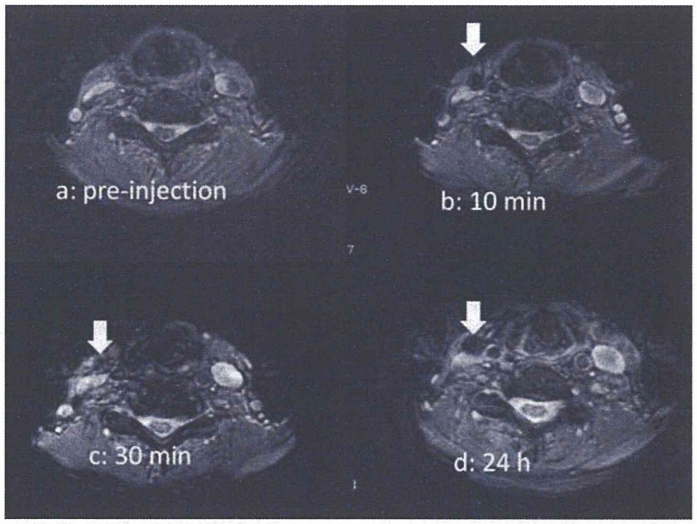

Figure 1. Arrows show sentinel nodes (SNs) detected with low signal intensity on fast-field echo T2*-weighted images in the right, level III region of the neck from 10 min to 24 h after injection using a 3.0 Tesla magnetic resonance (MR) imaging system; (a) pre-injection, and (b) 10 min, (c) 30 min, (d) 24 h after injection. Contrast effect by ferucarbotran (a superparamagnetic iron oxide) was detected at 10 min and persisted for 24 h.

the 10 min time point and persisted for 24 h (Figure 1: a, pre-injection; b, 10 min; c, 30 min; d, 24 h). The lymph nodes themselves were more clearly visualized in the 24 h coronal images with FFE T1-weighted image (FFE-T1WI) sequences than in any of the other image sequences (Figure 2). As time passed, larger numbers of lymph nodes, probably on and after the second echelon, were visualized as a sequentially connected appearance on the affected side of the neck and were also detected on the unaffected side (Table I and Figure 2). The SNs visualized in the 10 min image of interstitial MR lymphography were completely concordant with those visualized by ^{99m}Tc-radiocolloid lymphoscintigraphy and detected by a gamma probe in all cases (Table I and Figure 3). Iron incorporation into the SNs was confirmed by Berlin blue staining, revealing bright blue pigments inside the macrophages in the perifollicular sinus of the resected SN specimen (Figure 4).

SPIO, in volumes of 0.3, 0.15, and 0.1 ml, was injected in patients 1, 2, and 3, respectively. A transient, local, adverse response and tissue swelling at the injection site was observed in patients 1 and 2.

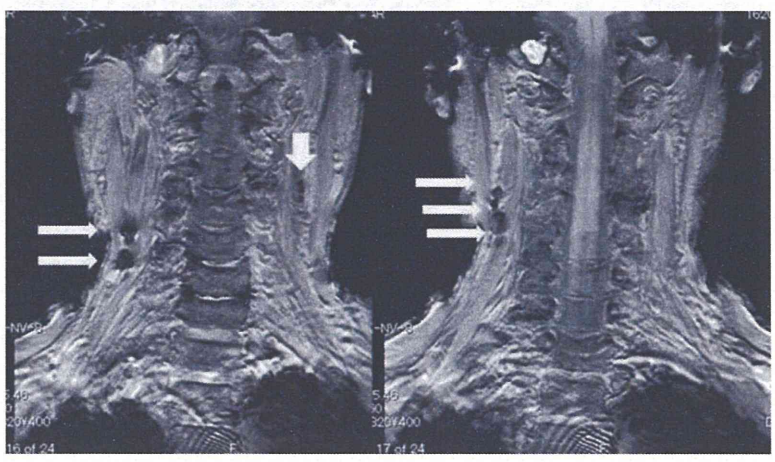

Figure 2. Arrows show lymph nodes detected with low signal intensity on fast-field echo (FFE) T1-weighted images at 24 h after injection into the affected (right) and the unaffected side. FFE T1-weighted image after 24 h showed the clearest images of the lymph nodes, but visualized larger numbers of additional lymph nodes, probably on and after the second echelon.

Table I. Patient characteristics and number of detected sentinel nodes.

				Radioisotope				MR lymphography with SPIO			
				Scintigraphy		Gamma probe		10 min		24 h	
Patient no.	Age (years)	Sex	T stage	Right	Left	Right	Left	Right	Left	Right	Left
1	86	F	2	1	0	1	0	1	0	9	2
2	52	M	2	3	0	3	0	3	0	>20	3
3	72	F	2	3	0	3	0	3	0	9	1

The sentinel lymph nodes visualized at 10 min image by interstitial magnetic resonance (MR) lymphography with superparamagnetic iron oxides (SPIOs) were completely concordant with those visualized by ^{99m}Tc-radiocolloid lymphoscintigraphy and detected by a gamma probe in all cases.

Representative case: patient 2

A 52-year-old female was referred to our hospital with a white ulcer (3 cm in diameter) in the right margin of her tongue. She was diagnosed with clinical T2N0M0 tongue cancer. SPIO, 0.15 ml, was injected into the right side of her tongue, as described earlier. Mild swelling was observed on the right side of the tongue 1 h after SPIO injection, but quickly resolved without any medication.

SNs were clearly visualized as low signal intensity structures in the 10 min FFE T1- and T2*-weighted MR images at levels IB, IIA, and III on her right side. The SNs detected in the 10 min FFE T1-weighted MR images were completely concordant with those detected by SPECT/CT, using radiocolloids, in the right, level IB, IIA, and III regions (Figure 3a–f). The SNs were visualized more clearly in the 24 h coronal images with FFE-T1WI sequences than in any other image sequences. Over 20 nodes were visualized with a long strand-like appearance on the right side of the neck and 3, on the left side, in the 24 h FFE T1WIs (Table I). The SN detected by a gamma probe during the surgical operation was located in the right, level IB, IIA, III region and the same SN was visualized by interstitial MR lymphography and SN SPECT/CT. Histological examination of the frozen tissue revealed a micrometastasis in the right, level IIA SN. Right, level IV region neck dissection was added to the originally scheduled right supraomohyoid neck dissection. The pathological evaluation of the neck dissection

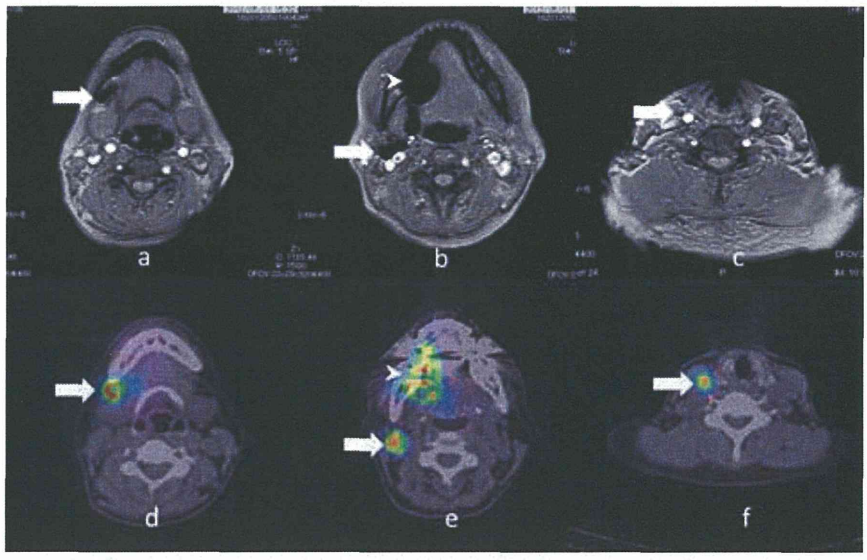

Figure 3. Arrows show sentinel nodes (SNs) in the right, level IB (a, d), IIA (b, e), III (c, f) region of the neck. SNs detected on fast-field echo (FFE) T1-weighted images at 10 min after injection of superparamagnetic iron oxides were completely concordant with those detected by single photon emission computed tomography (SPECT)/computed tomography (CT) using radiocolloids in the right, level IB, IIA, III region. Arrowhead shows injected site of the tongue. Although streak artifacts were seen around the injection site, they did not impair detection of SNs near the injection site. (a, b, c: FFE T1-weighted images at 10 min; d, e, f: SPECT-CT image of ^{99m}Tc-radiocolloid).

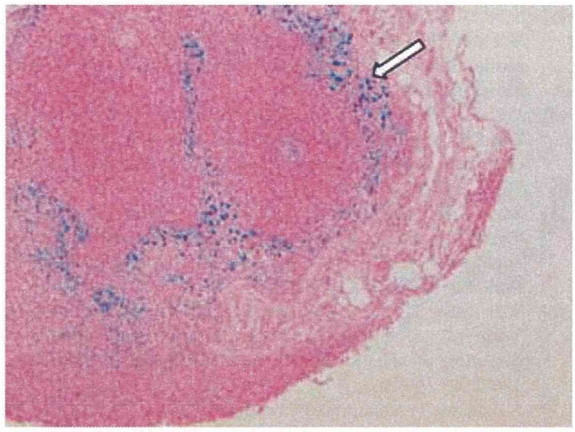

Figure 4. Bright blue pigments (arrow) indicating phagocytosis of iron particles derived from the injected superparamagnetic iron oxides, which were ingested by macrophages in the perifollicular sinus of the sentinel node (Berlin blue staining; 100 × magnification).

specimen and resected SN in paraffin embedded sections was as follows: right level IA (0/4), SN [IB] (0/1), IB (0/1), SN [IIA] (1/1), IIA (0/8), SN [III] (0/1), III (0/7), IV (0/3). (A/B; A = the number of lymph nodes with histopathologically proven metastasis, B = the number of lymph nodes dissected per anatomic neck level.) The patient was diagnosed with pathological T2N1 in the final stage. Iron incorporation into the resected SNs [IB, IIA, III] was also confirmed by the pathological examination.

Discussion

To the best of our knowledge, this is the first report of human SN detection using two techniques, interstitial MR lymphography using SPIO and ^{99m}Tc-radiocolloid lymphoscintigraphy, in patients with tongue cancer.

Although the usefulness of SNB in patients with head and neck cancer (clinical N0) is gaining popularity in clinical settings, SNB is only commonly used at a limited number of institutions. There are some concerns about the management of SNB using ^{99m}Tc-radiocolloid scintigraphy in patients with head and neck cancer because of its drawbacks, such as the shine-through phenomenon, and the necessity for an expensive gamma probe.

The use of radionuclides in Japan is strictly limited to designated areas. In contrast, no such limitations are associated with the use of SPIO, a commercially available contrast agent that was originally developed for use in the diagnosis of hepatocellular carcinoma. Generally, superparamagnetic nanoparticles are sequestered by phagocytic Kupffer cells in the liver and in the normal reticuloendothelial system (RES). Several researchers have reported that interstitial MR lymphography yields excellent results in the detection of SNs due to the presence of RES in the lymph nodes. The principal effect that SPIO nanoparticles have on MRIs is on T2* relaxation. Therefore, the MRIs are usually performed using T2/T2*-weighted sequences because of the tissue signal loss due to the effects of the iron oxide core. Negative contrast enhancement on T1-weighted images can also be seen with ferucarbotran nanoparticles.

The diameters of ferucarbotran and ^{99m}Tc-phytate particles are approximately 45–60 nm and 200–400 nm, respectively [12,13]. Interstitial MR lymphography using ferucarbotran was able to visualize a large number of lymph nodes, probably due to the smaller particle size and negative charge that may have resulted in increased phagocytosis. In the present study, SPIO incorporation by phagocytosis into the SNs was successfully demonstrated by Berlin blue staining of the resected node specimens.

The optimal timing for detection of SNs using interstitial MR lymphography with SPIO is yet to be determined. The first echelon node was clearly visualized at 10 min after interstitial administration of SPIO, concordant with the results of the ^{99m}Tc-radiocolloid lymphoscintigraphy. Thus, a 10 min image in interstitial MR lymphography with ferucarbotran seems to be optimal for SN detection.

The degree of incorporation of SPIO particles and their retention in phagocytic cells is dose dependent, and these compounds accumulate slowly and continuously over more than 5 h [14–16]. With regard to SN detection, the use of smaller sized SPIO nanoparticles is probably disadvantageous because of the rapid migration of the nanoparticles. However, the use of smaller size nanoparticles makes tracing the lymphatic routes from the injected sites to the SNs easier because multiple lymphatic channels can exist.

A local adverse response, tissue swelling at the injection site, was observed in two patients. Although this problem has yet to be solved, the adverse effect may depend on the volume of SPIO injected. Prevention of this side effect may require that the total dose does not exceed approximately 3 mg of ferucarbotran iron per 0.1 ml of undiluted Resovist™.

The shine-through phenomenon is a major limitation for the use of radiocolloids in SN detection, especially in submental lymph nodes, near the injection site. Although streak artifacts were seen around the injection sites in MR imaging with SPIO, they did not impair detection of SNs near the injected site, compared with imaging using radiocolloids, where such streaking was considered acceptable.

Interstitial MR lymphography has excellent spatial resolution that can help surgeons detect SNs during

surgery. Furthermore, several researchers have reported that a sensitive, hand-held magnetometer was as good for detecting SNs during surgery as the blue dye method is for lung and breast cancer [7,8]. The hand-held magnetometer is currently under development as a commercially available product. In the near future, if both preoperative MR lymphography and intraoperative detection using a magnetometer become available, SPIO could serve as one of the alternatives to radiocolloids for SN detection in patients with head and neck cancer. Furthermore, SPIO can be injected intraoperatively, which has the potential to eliminate the need for another preoperative procedure for detecting SNs.

In conclusion, interstitial MR lymphography with SPIO was a useful tool with high spatial resolution for SN detection in tongue cancer patients. The results indicated that further studies are warranted, as this novel method may replace the current scintigraphic technique.

Acknowledgments

The authors acknowledge the contribution of Osamu Matsubara, MD, PhD and Kosuke Miyai, MD, for their technical assistance during staining and their valuable comments for histology discussed in this manuscript. This research was supported by Health and Labor Sciences Research Grant for Clinical Cancer Research (H21-Gannrinshou-Ippan-016) from the Ministry of Health, Labor and Welfare, Japan. A summary of this manuscript was presented at Collegium Oto-Rhino-Laryngologicum Amicitiae Sacrum in August 29, 2012 in Rome, Italy.

Declaration of interest: The authors report no conflicts of interest. The authors alone are responsible for the content and writing of the paper.

References

[1] Kosuda S, Kusano S, Kohno N, Ohno Y, Tanabe T, Kitahara S, et al. Feasibility and cost-effectiveness of sentinel lymph node radiolocalization in stage N0 head and neck cancer. Arch Otolaryngol Head Neck Surg 2003;129: 1105–9.

[2] Tomifuji M, Shiotani A, Fujii H, Araki K, Saito K, Inagaki K, et al. Sentinel node concept in clinically N0 laryngeal and hypopharyngeal cancer. Ann Surg Oncol 2008;15:2568–75.

[3] Stoeckli SJ, Pfaltz M, Ross GL, Steinert HC, MacDonald DG, Wittekind C, et al. The second international conference on sentinel node biopsy in mucosal head and neck cancer. Ann Surg Oncol 2005;12:919–24.

[4] Paleri V, Rees G, Arullendran P, Shoaib T, Krishman S. Sentinel lymph node biopsy in squamous cell cancer of the oral cavity and oral pharynx: a diagnostic meta-analysis. Head Neck 2005;27:739–47.

[5] Stark DD, Weissleder R, Elizondo G, Hahn PF, Saini S, Todd LE, et al. Superparamagnetic iron oxide: clinical applications as a contrast agent for MR imaging of the liver. Radiology 1988;168:297–301.

[6] Weissleder R, Hahn PF, Stark DD, Elizondo G, Saini S, Todd LE, et al. Superparamagnetic iron oxide: enhanced detection of splenic tumors with MR imaging. Radiology 1988;169:399–403.

[7] Nakagawa T, Minamiya Y, Katayose Y, Saito H, Taguchi K, Imano H, et al. A novel method for sentinel lymph node mapping using magnetite in patients with non-small cell lung cancer. J Thorac Cardiovasc Surg 2003;126:563–7.

[8] Shiozawa M, Lefor AT, Hozumi Y, Kurihara K, Sata N, Yasuda Y, et al. Sentinel lymph node biopsy in patients with breast cancer using superparamagnetic iron oxide and a magnetometer. Breast Cancer 2012;Jan13Epub ahead of print.

[9] Torchia MG, Nason R, Danzinger R, Lewis JM, Thlivertis JA. Interstitial MR lymphography for the detection of sentinel lymph nodes. J Surg Oncol 2001;78:151–6.

[10] Kitamura N, Kosuda S, Araki K, Tomifuji M, Mizokami D, Shiotani A, et al. Comparison of animal studies between interstitial magnetic resonance lymphography and radiocolloid SPECT/CT lymphoscintigraphy in the head and neck region. Ann Nucl Med 2012;26:281–5.

[11] Robbins KT, Clayman G, Levine PA, Medina J, Sessions R, Shaha A, et al. Neck dissection classification update: revisions proposed by the American Head and Neck Society and the American Academy of Otolaryngology-Head and Neck Surgery. Arch Otolaryngol Head Neck Surg 2002; 128:751–8.

[12] Nomori H, Ohba Y, Yoshimoto K, Shibata H, Mori T, Shiraishi S, et al. Difference of sentinel lymph node identification between tin colloid and phytate in patients with non-small cell lung cancer. Ann Thorac Surg 2009;87: 906–10.

[13] Wang YX. Superparamagnetic iron oxide based MRI contrast agents: current status of clinical application. Quant Imaging Med Surg 2011;1:35–40.

[14] Raynal I, Prigent P, Peyramaure S, Najid A, Rebuzzi C, Corot C. Macrophage endocytosis of superparamagnetic iron oxide nanoparticles. Mechanisms and comparison of ferumoxides and ferumoxtran-10. Invest Radiol 2004;39: 56–63.

[15] Sun R, Dittrich J, Le-Huu M, Mueller MM, Bedke J, Kartenbeck J, et al. Physical and biological characterization of superparamagnetic iron oxide- and ultrasmall superparamagnetic iron oxide-labeled cells: a comparison. Invest Radiol 2005;40:504–13.

[16] Raynal I, Prigent P, Peyramaure S, Najid A, Rebuzzi C, Corot C. Macrophage endocytosis of superparamagnetic iron oxide nanoparticles. Invest Radiol 2004;39:56–63.

Acta Oto-Laryngologica, 2012; Early Online, 1–5

informa
healthcare

ORIGINAL ARTICLE

Platinum concentration in sentinel lymph nodes after preoperative intra-arterial cisplatin chemotherapy targeting primary tongue cancer

TOMOHIRO SAKASHITA[1], AKIHIRO HOMMA[1], NOBUHIKO ORIDATE[1], SEIGO SUZUKI[1], HIROMITSU HATAKEYAMA[1], SATOSHI KANO[1], TAKATSUGU MIZUMACHI[1], DAISUKE YOSHIDA[2], NORIYUKI FUJIMA[2] & SATOSHI FUKUDA[1]

[1]*Department of Otolaryngology-Head & Neck Surgery and* [2]*Department of Radiology, Hokkaido University Graduate School of Medicine, Sapporo, Japan*

Abstract

Conclusion: We conclude that intra-arterially injected cisplatin passed via lymph flow into sentinel nodes (SNs) as the platinum concentration in the SNs was higher than that in the non-sentinel nodes (NSNs). It is possible that preoperative intra-arterial chemotherapy targeting primary cancer also has a therapeutic effect on subclinical metastatic SNs. *Objectives*: Intra-arterial chemoradiotherapy has been reported to be effective against not only primary tumors but also nodal metastases. We considered the hypothesis that intra-arterially injected cisplatin passed via lymph flow into regional nodes. This study aimed to investigate intra-arterially injected cisplatin distribution to regional nodes by comparing platinum concentrations in SNs and NSNs. *Methods*: Five patients with T1-2 N0 tongue cancer were treated with preoperative intra-arterial chemotherapy (cisplatin, 100 mg/m^2) targeting primary cancer. Partial glossectomy together with SN biopsy and elective neck dissection were performed 2 weeks after intra-arterial chemotherapy. Platinum concentrations in the lymph nodes were measured using a Zeeman atomic absorption spectrometer. *Results*: Thirteen SNs were harvested together with eight NSNs from the areas adjacent to the SNs. Platinum concentrations were then measured, revealing a significant difference in platinum concentration between the SNs and the NSNs (mean ± SD, 0.682 ± 0.246 μg/g vs 0.506 ± 0.274 μg/g; $p = 0.049$).

Keywords: *Nodal metastasis, preoperative chemotherapy, RADPLAT*

Introduction

Intra-arterial chemotherapy and concurrent radiotherapy (RADPLAT) has been reported to be effective for head and neck squamous cell carcinomas (HNSCC) [1,2]. RADPLAT has a high impact on the primary site, and some reports have shown high nodal control rates for RADPLAT as well [3–5]. However, the mechanism by which intra-arterially injected cisplatin is distributed to the regional lymph nodes remains to be clarified. Therefore, we considered the hypothesis that intra-arterially injected cisplatin passed via lymph flow into the regional lymph nodes.

Recently, the concept of sentinel lymph node (SN) was established for HNSCCs, particularly for oral cancer [6–8]. This study aimed to investigate intra-arterially injected cisplatin distribution to the regional nodes by comparing platinum concentrations in SNs and non-sentinel lymph nodes (NSNs).

Material and methods

Patients and pretreatment evaluation

Since 2010, five patients with tongue cancers were diagnosed clinically as T1-2 N0 and were treated in our institution. Informed consent for the current

Correspondence: Tomohiro Sakashita, Department of Otolaryngology-Head and Neck Surgery, Hokkaido University Graduate School of Medicine, Kita 15, Nishi 7, Kita-ku, Sapporo 060-8638, Japan. Tel: +81 11 707 3387. Fax: +81 11 717 7566. E-mail: t-sakashita@med.hokudai.ac.jp

(Received 29 February 2012; accepted 22 March 2012)

ISSN 0001-6489 print/ISSN 1651-2251 online
DOI: 10.3109/00016489.2012.680494

clinical study was obtained from all five patients. Clinical staging was determined using computed tomography (CT) scanning, magnetic resonance (MR) imaging, positron emission tomography (PET)-CT scanning, and clinical examination by multiple specialists in head and neck surgery, radiology, and dentistry. Tumors were classified according to the American Joint Committee on Cancer (AJCC) staging system (7th edition, 2010). Four patients were classified as T2N0, and the remaining patient (case 1) was classified as T1N0 (Table I).

Approval for this study was obtained from the institutional review board at Hokkaido University. Completion of the survey was considered as implied consent for participation.

Preoperative chemotherapy

Intra-arterial cisplatin chemotherapy was performed for all five patients, using Seldinger's technique. Cisplatin was administered at a dose of 100 mg/m^2, and was injected rapidly (median 0.4 ml/s; mean 0.5 ml/s) to the lingual artery on the primary tumor involved side. Sodium thiosulfate (24 g/body) was simultaneously administered intravenously for neutralization. We performed partial glossectomy together with SN biopsy and elective neck dissection 2 weeks after the intra-arterial cisplatin chemotherapy.

Sentinel node scintigraphy

On the day before surgery day, we injected ^{99m}Tc-labeled phytate 75 mBq (1 ml) to the peri-primary tumor site and SN scintigraphy was performed 1 h after injection. Five surfaces (posterior to anterior, two transverse lines, and two oblique lines) were scanned using a gamma camera. The scanning of one surface took 5 min for the detection of radioactive points and imaging.

Surgical treatment

Partial glossectomy was performed within 18 h after the ^{99m}Tc-labeled phytate injection. We performed SN biopsy and elective neck dissection (level I, II, III on disease side) following glossectomy. A C-Trak collimated gamma probe (model CW3000; Carewise Medical Corp., Morgan Hill, CA, USA) was used for detecting radioactivity and measuring the over-threshold counts for 10 s. Radioactive nodes with counts that were 10 times higher than the background counts were recorded as SNs. SNs were analyzed pathologically at 2 mm intervals and sliced into 4 μm thick sections, and diagnosed using cytokeratin immunochemical staining (AE1/AE3). Histopathological degenerative change in metastatic lymph nodes after preoperative chemotherapy was evaluated using the histological criteria described in a previous report [9]. We harvested one NSN as a control from one area adjacent to the harvested SN.

Measurement of platinum concentration

We measured platinum concentrations in the primary tumors, SNs, and NSNs using a polarized Zeeman atomic absorption spectrometer (Model 170-70; Hitachi Ltd, Tokyo, Japan). Primary tumor tissues and node tissues were cut into 1 mm blocks. These specimens were digested at 176°F for 5 h using nitric acid and were chelated with sodium diethyldithiocarbamate. After chloroform extraction, these specimens were available for atomic absorption spectrometry.

Statistics

A mixed effect model was applied for comparison of the platinum concentrations in SNs and NSNs; an unpaired *t* test was applied when the platinum concentrations of two unpaired groups were compared.

Results

Treatment outcomes

All five patients underwent preoperative intra-arterial cisplatin infusion to the lingual artery on the tumor

Table I. Patient characteristics and number of sentinel nodes (SNs).

Case no.	Age (years)	Sex	Primary site	TN stage	Size (mm)	Depth (mm)	Cisplatin dose (mg/m^2)	No. of SNs
1	61	M	Tongue	T1N0	12 × 12	8	100	3
2	35	M	Tongue	T2N0	20 × 10	10	100	4
3	62	F	Tongue	T2N0	22 × 15	9	100	4
4	59	M	Tongue	T2N0	28 × 14	9	100	1
5	81	F	Tongue	T2N0	22 × 15	10	80	1

involved side. In cases 1–4, cisplatin was administered successfully at a dose of 100 mg/m^2. In case 5, the cisplatin dose was 80 mg/m^2 because of the patient's advanced age (81 years). Partial glossectomy together with SN biopsy and elective neck disssections were performed successfully 2 weeks after preoperative intra-arterial chemotherapy in all five cases. There were no adverse events after preoperative intra-arterial chemotherapy or after surgical treatments in any of the five cases. Multiple metastatic SNs were diagnosed pathologically in case 2. We performed postoperative radiation therapy (60 Gy/30 fr) with concomitant weekly cisplatin (40 mg/m^2) chemotherapy for case 2.

Sentinel node detection and pathological findings

We detected and harvested 13 SNs on the primary tumor involved side, using gamma camera and gamma probe. We also harvested eight NSNs from the areas adjacent to the harvested SNs. No SNs were detected on the contralateral side in any of five cases. Nodal metastases were observed pathologically in 7 of the 13 SNs. However, there were no metastases in the eight NSNs nor in any of the other lymph nodes included in the neck dissection specimens.

In three of seven metastatic SNs, degenerative changes (e.g. swelling of tumor cell, cytolysis, and partial necrosis) were observed histopathologically. However, viable tumor cells and tumor structures remained. In the remaining four metastatic SNs, tumor nests were very small and histopathological degenerative changes were hardly seen.

Platinum concentrations

Platinum concentrations were measured, revealing a significant difference in platinum concentration between the primary site and lymph node (mean ± SD, 1.978 ± 0.807 μg/g vs 0.615 ± 0.265 μg/g; $p < 0.001$). Table II shows results for platinum concentration.

The platinum concentrations in the SNs and NSNs were 0.682 ± 0.246 μg/g and 0.506 ± 0.274 μg/g, respectively. There was a significant difference between the platinum concentration in the SNs and that in the NSNs ($p = 0.049$, Figure 1).

Platinum concentrations in the metastatic SNs ($n = 7$) and non-metastatic SNs ($n = 6$) were 0.645 ± 0.245 μg/g and 0.724 ± 0.263 μg/g, respectively. There was no significant difference in platinum concentration between metastatic SNs and non-metastatic SNs ($p = 0.293$).

Clinical outcomes

All five patients are still alive without disease. There has been no primary site or regional recurrence in any of the five cases. The median of the observation period was 9 months (range 7–19 months, mean 12.2 months).

Table II. Summary of platinum concentrations.

	Sentinel nodes			Non-sentinel nodes			Primary tumor
Case no.	Region	Platinum concentration (μg/g)	Metastasis	Region	Platinum concentration (μg/g)	Metastasis	Platinum concentration (μg/g)
1	Ib	0.682	–	Ib	0.422	–	2.650
		0.376	+				
	IIa	0.794	–	IIa	0.455	–	
2	Ib	0.350	+	Ib	0.070	–	1.030
	IIa	0.370	–	IIa	0.570	–	
		0.620	+				
		0.560	+				
3	Ib	0.830	+	Ib	0.470	–	1.180
	IIa	1.150	–	IIa	0.530	–	
		0.790	–				
		0.560	–				
4	IIa	1.030	+	IIa	1.070	–	2.370
5	IIa	0.750	+	IIa	0.460	–	2.660
Mean ± SD		0.682 ± 0.246			0.506 ± 0.274		1.978 ± 0.807

SD, standard deviation.

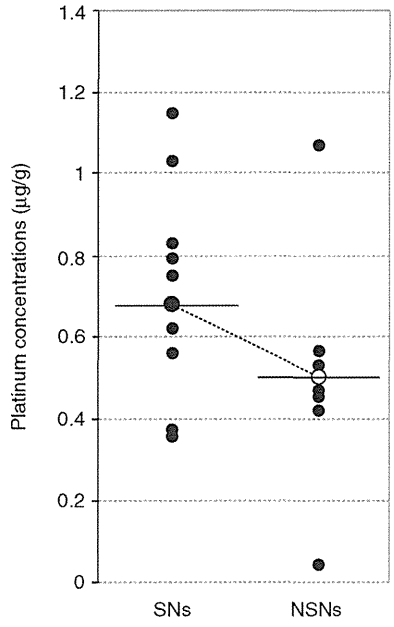

Figure 1. Data plots of platinum concentrations. NSNs, non-sentinel lymph nodes; SNs, sentinel lymph nodes.

Discussion

The presence of nodal metastasis in oral cancer is one of the most important prognostic factors and is crucial in making decisions regarding postoperative radiation treatment and follow-up. Even in patients with no clinical evidence of lymph node metastasis, there is a high incidence of occult metastasis, which ranges from 10% to 50% depending on the primary tumor characteristics including tumor subsite, T stage, and depth of invasion [10–14]. Additional treatment is not always successful in cases where subclinical nodal metastasis emerges clinically after initial treatment. Therefore, early detection of subclinical nodal metastasis and treatment of subclinical nodal metastasis are important and are considered to contribute to the clinical outcomes.

It is considered that deep invasion of the primary tumor is an important prognostic factor for nodal metastasis and recurrence. A depth of invasion of over 4 or 5 mm has been reported to be a risk factor [15,16]. The depth of invasion of the primary tumor in all five cases in our study was greater than 8 mm. Although all five of our cases were clinically diagnosed as N0, metastases in the SNs were observed pathologically in all five cases. We therefore reconfirmed that depth of invasion of the primary tumor was an important risk factor for subclinical nodal metastasis.

SN biopsy is considered a useful approach for the detection of subclinical nodal metastasis in patients diagnosed clinically as N0, and the efficacy of SN biopsy was reported and established for patients with oral cancer [6–8].

The application of SN biopsy after intra-arterial chemotherapy was reported by Kovács et al. [17], who concluded that lymphatic drainage was not significantly altered after intra-arterial chemotherapy targeting the primary tumor. SN biopsy following intra-arterial chemotherapy was, therefore, considered feasible.

Taking the above factors into consideration, preoperative intra-arterial chemotherapy for patients with deeply invasive primary tumors might be expected to be an effective treatment for not only the primary tumor but also subclinical nodal metastasis. Therefore, we investigated preoperative intra-arterial chemotherapy for patients with T1-2 N0 tongue cancers treated in our institute since 2010.

It was reported that intra-arterial cisplatin chemotherapy with concurrent radiotherapy is effective against primary tumors [1,2]. Some reports have also proven the therapeutic efficacy of RADPLAT for neck disease. The nodal control rate of RADPLAT with or without salvage neck dissection was reported to be 87.1–91% [3–5]. Robbins et al. [5] reviewed 240 patients with HNSCC and nodal metastasis of which 84 underwent salvage neck dissection. On pathological examination of the neck dissection specimens, 50 patients (60%) were found to have no residual disease. From these reports, RADPLAT can be considered to be an effective treatment for not only primary tumors but also nodal metastases. We therefore considered the hypothesis that cisplatin injected into primary tumor by an intra-arterial approach passes via lymph flow into the regional lymph nodes.

Our findings of a higher platinum concentration in SNs than in NSNs support this hypothesis. In addition, histopathological degenerative changes were observed in three of seven metastatic SNs in our study. Based on the histopathological grading system used in the previous report, these histopathological changes were evaluated as grade I, which indicates initial anti-tumor effect and remaining tumor structures [9,18]. It is also possible that intra-arterial cisplatin chemotherapy targeting the primary tumor has a therapeutic effect on subclinical metastatic SNs. However, the results of our current study do not provide any evidence of clinical benefit. Further studies are needed to determine the clinical benefit of preoperative intra-arterial chemotherapy.

It was reported that a completely occupied metastatic node has no accumulation of tracer [19]. When the ratio of metastatic area in the lymph node was more than 90%, it was thought that the tracer could not flow into that lymph node. Therefore, it was

considered that intra-arterially injected cisplatin could not reach completely occupied metastatic SNs. The therapeutic efficacy of preoperative intra-arterial chemotherapy for completely occupied metastatic SNs has, therefore, not yet been clarified.

Conclusion

We found that the platinum concentration in SNs was higher than that in NSNs after preoperative intra-arterial cisplatin chemotherapy targeting the primary tumor. It is speculated that the intra-arterially injected cisplatin passes via lymph flow into the SNs. It is also possible that intra-arterial chemotherapy targeting the primary tumor has a therapeutic effect on subclinical metastatic SNs. The strategy of combined preoperative intra-arterial chemotherapy and SN biopsy could, therefore, afford clinical benefits to patients with subclinical metastatic nodes.

Acknowledgments

This study was supported by a Health and Labour Sciences Research Grant for Clinical Cancer Research (H21-Gannrinshou-Ippan-016) from the Ministry of Health, Labour and Welfare, Japan.

Declaration of interest: The authors report no conflicts of interest. The authors alone are responsible for the content and writing of the paper.

References

[1] Robbins KT, Kumar P, Regine WF, Wong FS, Weir AB 3rd, Flick P, et al. Efficacy of targeted supradose cisplatin and concomitant radiation therapy for advanced head and neck cancer: the Memphis experience. Int J Radiat Oncol Biol Phys 1997;38:263–71.

[2] Homma A, Oridate N, Suzuki F, Taki S, Asano T, Yoshida D, et al. Superselective high-dose cisplatin infusion with concomitant radiotherapy in patients with advanced cancer of the nasal cavity and paranasal sinuses: a single institution experience. Cancer 2009;115:4705–14.

[3] Robbins KT, Wong FS, Kumar P, Hartsell WF, Vieira F, Mullins B, et al. Efficacy of targeted chemoradiation and planned selective neck dissection to control bulky nodal disease in advanced head and neck cancer. Arch Otolaryngol Head Neck Surg 1999;125:670–5.

[4] Sakashita T, Homma A, Oridate N, Hatakeyama H, Kano S, Mizumachi T, et al. Evaluation of nodal response after intra-arterial chemoradiation for node-positive head and neck cancer. Eur Arch Otorhinolaryngol 2011 Nov 1 [Epub ahead of print].

[5] Robbins KT, Doweck I, Samant S, Vieira F. Effectiveness of superselective and selective neck dissection for advanced nodal metastases after chemoradiation. Arch Otolaryngol Head Neck Surg 2005;131:965–9.

[6] Civantos FJ, Moffat FL, Goodwin WJ. Lymphatic mapping and sentinel lymphadenectomy for 106 head and neck lesions: contrasts between oral cavity and cutaneous malignancy. Laryngoscope 2006;112(3 Pt 2 Suppl 109):1–15.

[7] Jefferson GD, Sollaccio D, Gomez-Fernandez CR, Civantos F Jr. Evaluation of immunohistochemical fine sectioning for sentinel lymph node biopsy in oral squamous cell carcinoma. Otolaryngol Head Neck Surg 2011;144:216–19.

[8] Yoshimoto S, Hasegawa Y, Matsuzuka T, Shiotani A, Takahashi K, Kohno N, et al. Sentinel node biopsy for oral and laryngopharyngeal squamous cell carcinoma: a retrospective study of 177 patients in Japan. Auris Nasus Larynx 2012;39:65–70.

[9] Shimosato Y, Oboshi S, Baba K. Histological evaluation of effects of radiotherapy and chemotherapy for carcinomas. Jpn J Clin Oncol 1971;1:19–35.

[10] Hosal AS, Carrau RL, Johnson JT, Myers EN. Selective neck dissection in the management of the clinically node-negative neck. Laryngoscope 2000;110:2037–40.

[11] van den Brekel MW, van der Waal I, Meijer CJ, Freeman JL, Castelijns JA, Snow GB. The incidence of micrometastases in neck dissection specimens obtained from elective neck dissections. Laryngoscope 1996;106:987–91.

[12] Shah JP, Andersen PE. The impact of patterns of nodal metastasis on modifications of neck dissection. Ann Surg Oncol 1994;1:521–32.

[13] Vigili MG, Tartaglione G, Rahimi S, Mafera B, Pagan M. Lymphoscintigraphy and radioguided sentinel node biopsy in oral cavity squamous cell carcinoma: same day protocol. Eur Arch Otorhinolaryngol 2007;264:163–7.

[14] Ross GL, Soutar DS, Gordon MacDonald D, Shoaib T, Camilleri I, Roberton AG, et al. Sentinel node biopsy in head and neck cancer: preliminary results of a multicenter trial. Ann Surg Oncol 2004;11:690–6.

[15] Kane SV, Gupta M, Kakade AC, D'Cruz A. Depth of invasion is the most significant histological predictor of subclinical cervical lymph node metastasis in early squamous carcinomas of the oral cavity. Eur J Surg Oncol 2006;32:795–803.

[16] Liao CT, Lin CY, Fan KH, Wang HM, Ng SH, Lee LY, et al. Identification of a high-risk group among patients with oral cavity squamous cell carcinoma and pT1-2-N0 disease. Int J Radiat Oncol Biol Phys 2012;82:284–90.

[17] Kovács AF, Landes CA, Hamscho N, Döbert N, Menzel C. Pattern of drainage in sentinel lymph nodes after intra-arterial chemotherapy for oral and oropharyngeal cancer. J Oral Maxillofac Surg 2005;63:185–90.

[18] Ikushima I, Korogi Y, Ishii A, Hirai T, Yamura M, Nishimura R, et al. Superselective arterial infusion chemotherapy for squamous cell carcinomas of the oral cavity: histopathologic effects on metastatic neck lymph nodes. Eur Arch Otorhinolaryngol 2007;264:269–75.

[19] Matsuzuka T, Kano M, Ogawa H, Miura T, Tada Y, Matsui T, et al. Sentinel node mapping for node positive oral cancer: potential to predict multiple metastasis. Laryngoscope 2008;118:646–9.

日気食会報，64（3），2013

用 語 解 説

センチネルリンパ節

I. はじめに

早期の口腔癌N0例での潜在リンパ節転移率は20％程度で，欧米では頸部リンパ節の取り扱いは“wait and see”は薦められず，むしろ予防的に頸部郭清術を行うべきだという報告が多い。一方で，頸部郭清術の合併症として術後出血や下位脳神経麻痺，顔面の浮腫，リンパ液の貯留，知覚異常や神経障害などがあげられ，不必要な頸部郭清術を省略できればこれらの合併症を防ぐことができる。適切な症例に適切な頸部郭清術を行うための明確な指標が求められている。センチネルリンパ節（sentinel lymph node, SLN）はこの指標になり得ると考えられている。

II. センチネルリンパ節とは

SLNとは腫瘍から最初に転移するリンパ節のことであり，トレーサーと呼ばれる薬剤を腫瘍の周囲に注入すると，腫瘍からドレナージされる最初のリンパ節を同定でき，このリンパ節をSLNとみなす。SLNに転移がなければ他のリンパ節には転移がないと推定され，郭清術を行わなくてよいと考えられる（Fig. 1）。

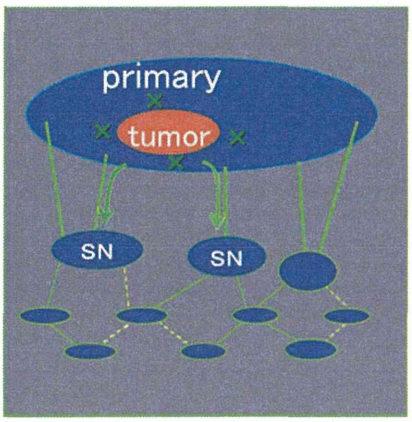

Fig. 1 センチネルリンパ節

III. センチネルリンパ節の歴史

Aristotleがリンパ管の観察を行い，1863年にVirchowが所属リンパ節の重要性を記している[1]。1939年に最も転移の生じやすいリンパ節の存在の報告がある[2]。1960年には耳下腺腫瘍における特定のリンパ節を迅速診断し頸部郭清術の適応を決める報告があり，このリンパ節を“sentinel lymph node”と定めたのが最初である[3]。手術中に使用可能なハンディタイプのガンマ線検出器が製品化され，1992年に悪性黒色腫，1994年に乳癌でSN生検が報告された。口腔癌では1996年に最初の報告がある[4]。現在，乳癌，悪性黒色腫ではSLN生検のEBMが確立されつつあり，口腔癌でも多施設研究が進行している。

IV. トレーサーについて

SNの検出に使用するトレーサーには，色素を用いる色素法と，ラジオアイソトープ（RI）を用いるRI法がある。色素法におけるトレーサーはイソサルファンブルーやサルファンブルーが用いられていたが，アナフィラキシーや発癌の報告があり，国内ではインドシアニングリーン（ICG）やインジゴカルミンなどが用いられている。頸部はリンパ節が透見し難いため色素法は頻用されていないが，ICGは近赤外線を励起する特徴があり，蛍光法として研究が進んでいる。

RI法のトレーサーはコロイド製剤が用いられる。コロイドの粒子径が小さいとリンパ管への移行は容易であるが，リンパ節から流出してしまうため，リンパ節への残留を考慮すると，粒子径は200～1000 nm程度が適切で，本邦では^{99m}Tc標識スズコロイドやフチン酸がよく用いられる。フチン自体はコロイドではないが体内のカルシウムと反応し300 nm前後のコロイドを形成する。トレーサーの種類の違いによるSNの平均個数は以前使用していたレニウムコロイド（粒子径：100 nm前後）が3.7個，現在使用しているフチン酸では2.3個であった。

V．センチネルリンパ節生検の方法

RI法でセンチネルリンパ節生検を行っている。^{99m}Tc標識フチン酸は74から34 MBqに調整し，腫瘍周囲の粘膜下4カ所に計0.4 ml注入する。トレーサー注入より2時間後にシンチカメラを使用してSLNの集積位置を確認する（Fig. 2）。注入部に残留した薬剤量はSLNに流入・蓄積する量より多いため，注入部に隣接したリンパ節の集積を確認するのが難しい。この現象をシャインスルーと呼ぶが，この対策として，1）注入部直上を鉛で遮蔽し頸部シンチグラフィ撮像する，2）SPECTCT（Fig. 2）を行う。術中には原発部位の切除を先行して行う。

VI．センチネルリンパ節生検のエビデンス

本邦7施設，計177症例のSLN生検術の実態調査を行った。同定率は口腔癌では98.1%，喉頭および下咽頭癌では100%となった。口腔癌157例の5年累積生存率は81.8%，喉頭および下咽頭癌20例では89.4%となった。偽陰性率は6.9%であった[5]。

VII．センチネルリンパ節生検の注意点

転移が明らかなリンパ節にはトレーサーの集積をきたさない場合がある。これは腫瘍がリンパ節内を占拠するとリンパの流入が途絶してしまうためで，SN生検はあくまで潜在転移を探索する手技である。

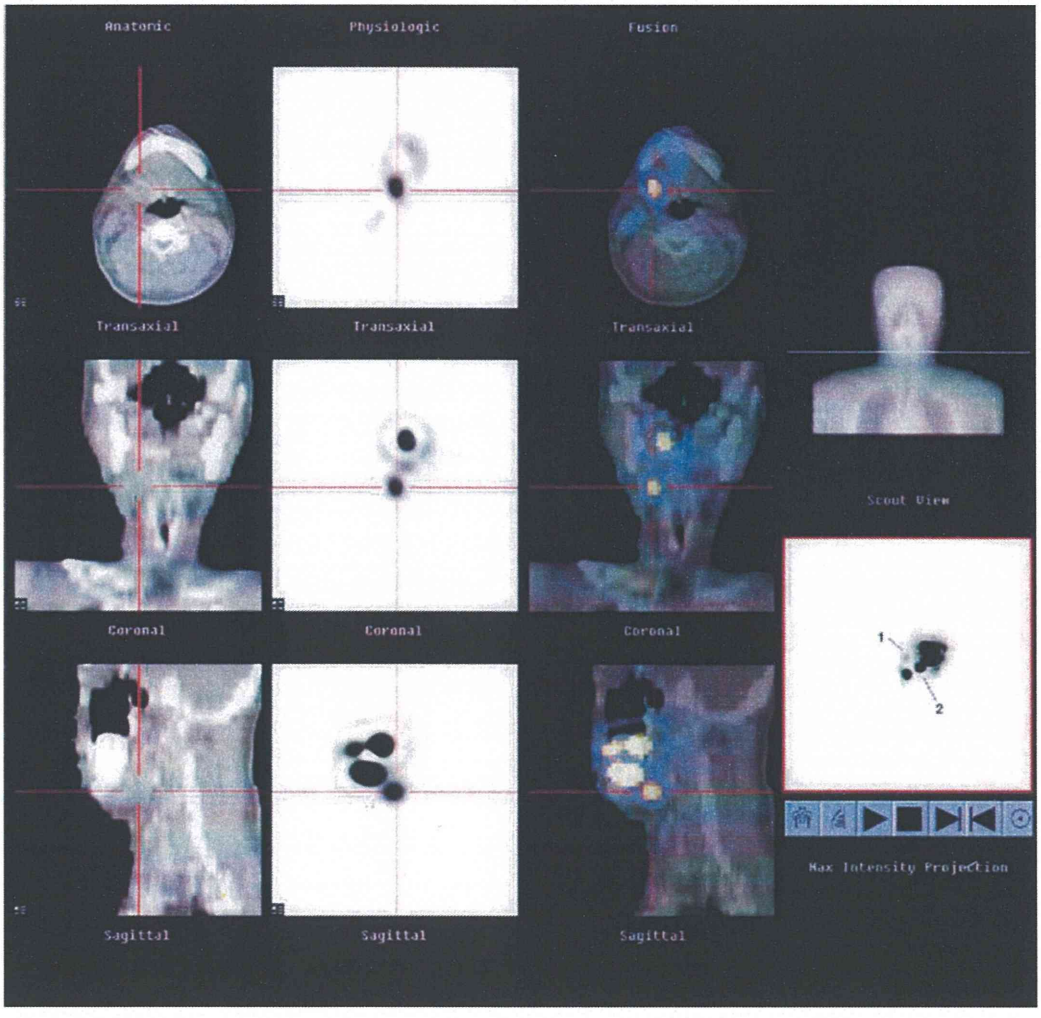

Fig. 2　シンチグラフィとSPECTCT

文　献

1）Borgstein P, Meijer S：Historical perspective of lymphatic tumour spread and the emergence of the sentinel node concept. Eur J Surg Oncol 24：85–89, 1998.
2）Gray JH：The relation of lymphatic vessels to the spread of cancer. Br J Surg 26：464–495, 1939.
3）Gould EA, Winship T, Philbin PH, et al：Observation on a "sentinel node" in cancer of the parotid. Cancer 13：77–78, 1960.
4）Alex JC, Krag DN：The gamma-probe-guided resection of radiolabeled primary lymph nodes. Surg Oncol Clin N Am 5：33–41, 1996.
5）Yoshimoto S, Hasegawa Y, Matsuzuka T, et al：Sentinel node biopsy for oral and laryngopharyngeal squamous cell carcinoma：A retrospective study of 177 patients in Japan. Auris Nasus Larynx 39：65–70, 2012.

（愛知県がんセンター中央病院 頭頸部外科
長谷川泰久，
福島県立医科大学医学部 耳鼻咽喉科　松塚　崇）

〈学 術 論 文〉

頭頸部領域における間質内 MR リンパ造影と放射性コロイドによる SPECT/CT リンパシンチグラフィ — 動物実験による比較検討

平成 23 年度厚生労働省科学研究費補助金 (H21-がん臨床-一般-016) による研究

防衛医科大学校放射線医学講座　小須田　茂、新本　弘
同　耳鼻咽喉科学教室　溝上　大輔、冨藤　雅之、荒木　幸二、塩谷　彰浩
国立がんセンター東病院　機能診断開発部　藤井　博史
慶應義塾大学医学部放射線治療科　北村　直人

はじめに

頭頸部癌患者の治療方針決定のために放射性コロイドを用いたセンチネルリンパ節生検 (sentinel lymph node biopsy, SLNB) の応用に関して報告がみられる[1~4]。SLNB は有用な手段となった。この方法によって、頭頸部外科医が無益で、不要な頸部郭清を避けられ、肩の疼痛といった術後合併症の発生を減少させることができる。

しかし、放射性コロイドを用いた SLNB はいくつかの欠点を有している。センチネルリンパ節が放射性コロイド注入部位の近傍に存在すると、その部位の高放射能によって生じる Shine-through 現象によってセンチネルリンパ節の同定が困難となる。

超常磁性酸化鉄 (superparamagnetic iron oxide, SPIO) はナノ粒子でマクロファージ、貪食細胞に取り込まれるため、マクロファージ画像製剤として使われる[5,6]。SPIO は T2 強調画像、T2* 強調画像で、強い陰性造影を生じる。間質内 MR リンパ造影はセンチネルリンパ節同定に優れた結果をもたらしたとの論文がある[7,8]。

この研究の目的は、動物モデルを用いて、放射性コロイドによる SPECT/CT リンパシンチグラフィと SPIO とガドキセト酸ナトリウムによる間質内 MR リンパ造影、という 2 つの手技をセンチネル描出能に関して比較評価することである。われわれの知る範囲では、この研究は頭頸部領域で 2 つの手技を比較した最初の研究である。

対象および方法

この研究で行ったすべての処置は実験動物の管理と使用のための当施設ガイドラインに遵守した。8 週齢の 23～27 g のオスのヌードマウス (BALB/c Slc-nu/nu)、21 匹を用いた。イソフルレインで麻酔し、実験前に動きを抑制するために固定した。呼吸同期は行わなかった。造影剤、放射性コロイド、のいずれも投与しない 3 匹のマウスをコントロールとして用いた。

[SPECT/CT リンパシンチグラフィ]

^{99m}Tc-フチン酸、0.02 mL、7.4 MBq を 6 匹のマウスの舌右縁、粘膜下に投与した。リンパ節 (センチネルリンパ節) を検出する目的で、局注後 30 分でリンパシンチグラフィを撮影し

た。動物用全身 SPECT/CT ハイブリッドスキャナー、NanoSPECT/CT (BIOSCAN Mediso., Washington, DC, USA) を用いた。われわれが用いた SPECT 装置は、9 ホールを有するピンホールコリメータを装着した 3 検出器を有している。ホール (孔) の大きさは直径 1.4 mm である。CT 撮影時の電圧、電流はそれぞれ 45 kV、177 microA で、ヘリカル CT 収集であった (図 1)。リンパ節描出能に関する最適な撮影時間に関する検討は、頭頸部領域ですでに確立されているために、行わなかった[1~4]。

図 1

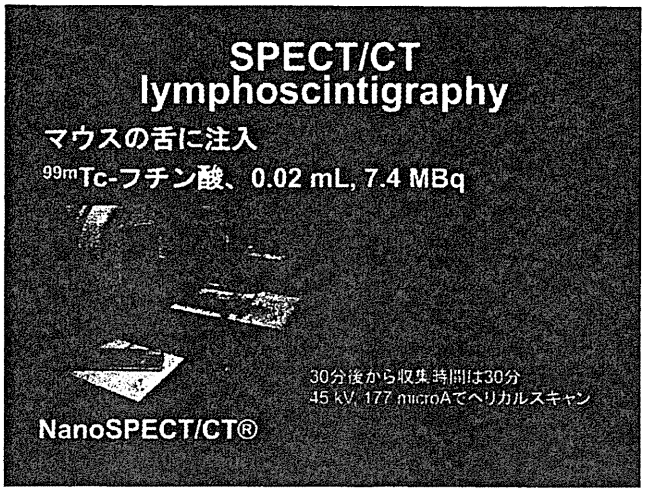

[間質内 MR リンパ造影]

センチネルリンパ節検出には Varian Unity INOVA 4.7 テスラ MRI 装置を用いた。コイルには、傾斜磁場コイル：6.5 ガウス/cm、送信コイル：Varian volume coil、16 cm、受信コイル：handmade surface coil、5 cm である。

パルスシークエンスは、3D gradient-echo: TR/TE＝0.02/0.004 s、field of view (FOV)＝80×40×40 mm、matrix size＝128×64×64、フリップ角 8 度、スピンエコー法：T1 強調画像 TR/TE＝0.4/0.014 s、FOV＝40×40 mm、matrix size＝256×256、スライス厚 1.3 mm、グラディエントエコー：T2*WI TR/TE＝0.02/0.008 s、FOV＝40×40 mm、matrix size＝256×256、スライス厚 1.3 mm、フリップ角 32 度である。

MRI 装置で収集された free induction decay (FID) データは 16 ビットフォーマットで表示された。データはフーリエ変換と MATLAB プログラム (Math Works Inc., Natick, Massachusetts, USA) を用いて処理された。

バイエル薬品 (Bayer Schering Pharma AG, Berlin, Germany) から提供された ferucarbotran (レゾビスト®) を粘膜下局注後、30 分、80 分、110 分、24 時間にてグラディエントエコー法の T2*WI が撮影された。局注の実際は、ferucarbotran、鉄として 0.279 mg、0.01 mL を 29 ゲージの針を有する 1 mL シリンジで 6 匹のマウスの舌右縁粘膜下に投与した。また、バイエル薬品から提供された gadoxetate disodium を 6 匹のマウスの舌右縁粘膜下局注後、10 分、20 分、30 分、40 分、50 分、60 分、70 分、80 分にて通常の T1WI が撮影された。gadoxetate disodium の投与量は 0.01 mL、0.363 mg であった。これらの投与量はこれまでに報告された研究[7,9]、および平成 23 年度厚生労働省科学研究費補助金 (H21-がん臨床-一般-016) による頭頸部

sentinel node navigation surgery 会議での個人的折衝によって決定された。

関心領域 (region of interest, ROI) は、カラー解剖アトラスを参照して左右の顎下リンパ節とバックグランドとしての頸部筋組織上に注意深く設定された[12~14]。時間信号強度グラフは、それぞれの ROI から作成された。さらに、これらのデータは商品化されたソフトウエア、ImageJ によって解析された。ROI の信号強度はバックグランドの信号強度で除することによって得られた。Ferucarbotran、gadoxetate disodium のいずれも、単純 MRI 像の信号強度を 1.0 として、上述のソフトウエアを用いて、時間信号強度グラフを作成した。Ferucarbotran、gadoxetate disodium を間質内注入後の経時的評価で良好な画像を得るための最適時間を検討した。

間質内 MR リンパ造影と放射性コロイドによる SPECT/CT リンパシンチグラムのリンパ節描出程度に関する読影実験が 10 年以上の経験を有する放射線科専門医で行われた。間質内 MR リンパ造影画像はコントロールマウスの画像と比較された。

間質内 MR リンパ造影と SPECT/CT リンパシンチグラムのリンパ節描出程度は 4 段階、すなわち、不良 (スコア 0)、可 (スコア 1)、良好 (スコア 2)、優良 (スコア 3) に分類され、3 名の読影医によって視覚的、主観的にスコア化された。

3 名のリンパ節描出程度の段階比較研究で、統計学的解析では、SPSS ソフトウエアを用いて、two-factor mixed design with repeated measures on one factor により有意差検定を行った。P 0.05 以下を統計的に有意差ありとした。

結　果

センチネルリンパ節はカラー表示 SPECT/CT 融合画像リンパシンチグラフィで良好に描出された。SPECT/CT 融合画像リンパシンチグラフィで描出されたリンパ節の個数は、それぞれ 3、3、5、6、3、4 であった (平均：4.0 リンパ節)。右側に 16 個、左側に 8 個であった。

コントロールマウスで正常顎下リンパ節は T2*WI でわずかに低信号として描出された。Ferucarbotran を用いた間質内リンパ造影では、局注後 30 分から 24 時間にわたり、左右顎下リンパ節は T2*WI で低信号として描出された。顎下リンパ節以外のリンパ節は T2*WI で描出されなかった。しかし、信号強度は徐々に低下したものの、gadoxetate disodium 局注後 10 分から 80 分までの間、顎下リンパ節のみが高信号として描出された。Shine-through 現象は ferucarbotran 間質内投与 T2*WI で、gadoxetate disodium 間質内投与 T1WI で、いずれも注入部位に認められた。

T2*WI での時間信号強度グラフは ferucarbotran 間質内投与 30 分で、顎下リンパ節信号強度は投与前に比較して約 1/2 に低下した (投与前を 1.0 として、右：0.43、左：0.61)。ferucarbotran 投与後 24 時間までに信号強度は徐々に低下した。右側の顎下リンパ節の信号強度は左側よりも低値であった (図 2)。

Gadoxetate disodium 間質内投与の T1WI で得られた時間信号強度グラフでは投与後 10 分で最高値 (投与前を 1.0 として、右側顎下リンパ節 1.43、左側顎下リンパ節 1.33) が観察され、投与後 80 分にわたり徐々に低下した。右側顎下リンパ節の信号強度は左側顎下リンパ節のそれよりも高値を示した (図 3)。

Ferucarbotran、gadoxetate disodium のいずれも、間質内 MR リンパ造影では 2 つのリンパ

図 2

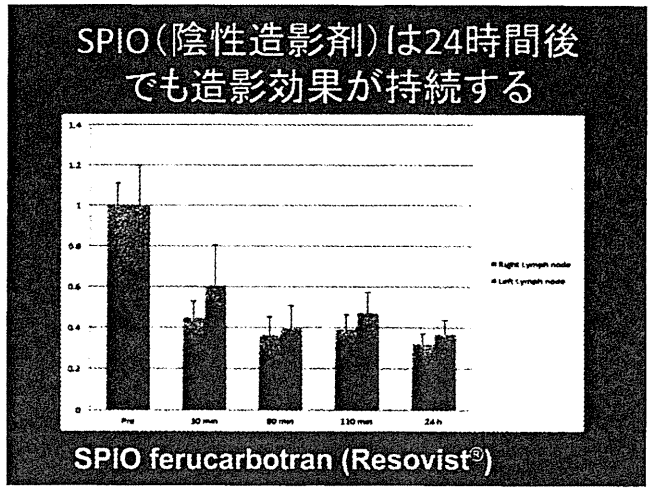

図 3

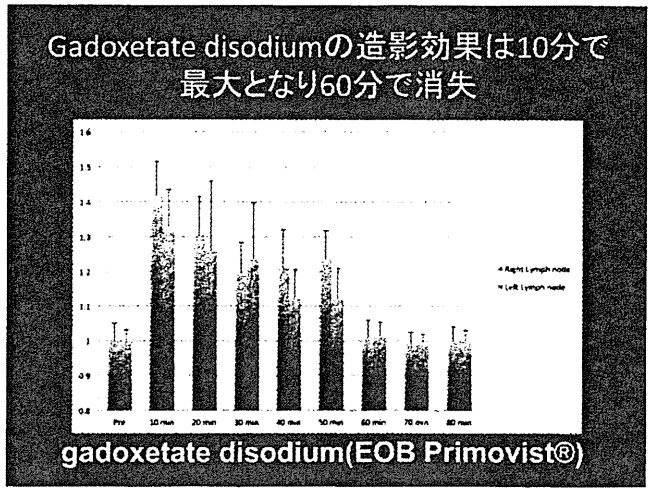

表 1

readers	MRI ferucarbotran mouse 1, 2, 3, 4, 5, 6	MRI gadoxetate disodium mouse 7, 8, 9, 10, 11, 12	SPECT/CT mouse 13, 14, 15, 16, 17, 18
reader A	G G G G F F	G G F G G G	E E G G E G
reader B	F F G F F F	G G G F F G	E E G G E E
reader C	F G G G F F	G G F F F G	E E E G E E

P: poor = 0, F: fair = 1, G: good = 2, E: excellent = 3

節（左右顎下リンパ節）のみが描出された（平均描出節数：2 リンパ節）。間質内 MR リンパ造影で描出されたリンパ節（左右顎下リンパ節）は SPECT/CT で描出されたリンパ節のうち、最も高い放射能を有したリンパ節に一致した。

3 名の読影医によるセンチネルリンパ節描出能に関する間質内 MR リンパ造影と、放射性コロイドによる SPECT/CT リンパシンチグラムの段階評価を表 1 に示す。その結果、SPECT/CT リンパシンチグラムが間質内 MR リンパ造影よりも優れた成績であった（表 1、図 4）。3 名の読影医による平均スコアは、SPIO ferucarbotran 間質内 MR リンパ造影 1.44、gadoxetate

図4

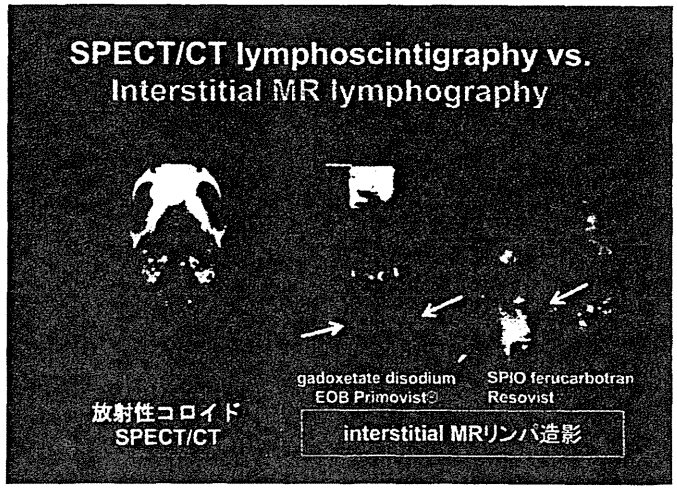

disodium 間質内 MR リンパ造影 1.67、SPECT/CT リンパシンチグラム 2.67 であった。このように、平均スコアにおいて SPECT/CT リンパシンチグラムと間質内 MR リンパ造影において統計学的有意差が認められた (two-factor mixed design with repeated measures on one factor: $p < 0.0002$)。

なお、注入部位とその周辺組織は腫脹、ferucarbotran で青褐色変化という所見が出現した。

考　察

N0 頭頸部癌患者における SLNB の有用性については徐々に臨床の場で認められるようになってきているが、ある一定の病院を除き世界で広く用いられているわけではない。加え得るに、^{99m}Tc 標識放射性コロイドを使用する場合の懸念がある。とくに、口腔底癌、舌癌、歯肉癌患者では、オトガイ下、顎下部リンパ節は shine-through 現象によってその検出に大きく影響を受ける。^{99m}Tc 標識放射性コロイドによる SLNB は適切なトレーニングと経験が要求される。舌癌患者における放射性コロイドによる SLNB の偽陰性率は比較的高く 8% であり、SLNB の実効性を損なう可能性があり、また、センチネルリンパ節概念にも矛盾するかもしれない[15]。

MRI 造影剤 SPIO ferucarbotran は肝臓イメージング製剤として開発された。Ferucarbotran の粒子径サイズは 60～200 nm である[16]。このサイズは肝 Kupffer 細胞に取り込まれるのに適した大きさで、T2WI と T2*WI で著明な信号低下をきたす。肝内腫瘍の検出に SPIO の有用性が多く報告されている。

われわれの検討では、4.7 テスラ MRI 装置で ferucarbotran、gadoxetate disodium のいずれも、間質内 MR リンパ造影で 2 つのリンパ節（左右顎下リンパ節）のみが描出された。1.0～3.0 テスラ MRI 装置でも、間質内 MR リンパ造影は可能であると思われる[8,9]。すべての pulse sequence で、注入側である右側顎下リンパ節は左側と比較して良好に描出され、時間信号強度グラフでも信号強度に左右差がみられたことから、右側顎下リンパ節がセンチネルリンパ節と思われた。舌癌患者での臨床報告でも、顎下リンパ節が高頻度に微小転移をきたすセンチネルリンパ節の一つである[1~4,15,17]。最近、gadolinium-diethylene triamine-pentaacetic acid (Gd-DTPA) の一種で、脂溶性 ethyl-oxy-benzyl 群である gadoxetate disodium が肝細胞特異製剤と

して用いられている[18]。SPIOと異なり、gadoxetate disodiumはナノ粒子ではない。Gadoxetate disodiumは間質内MRリンパ造影として優れた造影剤との報告があり、われわれの研究でも使用した[9]。リンパ節描出のための最適時間はこれまでの報告と一致した[7,9]。

画質に関しては、リンパ節を陽性描画するgadoxetate disodiumの方がferucarbotranよりも優れた結果を示した（表1）。しかし、gadoxetate disodiumはリンパ節からの洗い出しが速いという難点を有している。一般に、造影剤（鉄製剤）が急速に洗い出される場合、手術時体外から検知する手持ちmagnetmeterを使用するのが困難である一方、間質性MRリンパ造影を繰り返し行うことができる。Gadoxetate disodiumとは対照的に、SPIOの細胞内取り込みと保持の程度は、投与量に依存し、緩徐に、連続的に5時間以上かけて集積する[10]。Ultra-small SPIOと比較して、SPIOは大きさと陰イオンの関係から貪食能を有する細胞には取り込まれやすく、より高い集積性を示す[11,19]。

Shine-through現象は間質内MRリンパ造影でも認められた。造影剤を多量に投与したため縞状アーチファクトが注入部位周囲に認められた。マウスあたりの適正投与量を明確にする必要がある。われわれは、原液造影剤を使用したが、生理的食塩水で希釈するなどの対策は縞状アーチファクトを減じる可能性がある。

さらに、多量の造影剤が粘膜下に投与されたため、注入部位とその周辺組織は腫脹、ferucarbotranで青褐色変化という副作用が現れた。しかし、注入局所の有害事象は原発巣とともに切除されるために、大きな問題ではないと思われる。

異なる画像を比較し優劣をつけることはいつも困難に遭遇するが、臨床家による肉眼的段階評価は画像向上の糸口を与える。3人の読影医は間質内MRリンパ造影とSPECT/CTリンパシンチグラフィにおけるリンパ節描出そのものと画質を評価したが、SPECT/CTリンパシンチグラフィが間質内MRリンパ造影よりも優れた評点スコアであった。描出された平均リンパ節数は、間質内MRリンパ造影2.0、SPECT/CTリンパシンチグラフィ4.0であった。最高カウント数のリンパ節あるいは最初のechelonリンパ節に微小転移が必ずしもおこるとは限らないので[14]、間質内MRリンパ造影は微小リンパ節転移を見逃す可能性がある。腫瘍からのリンパ流が同時に2、3ルートを介して発生することがありうるのでリンパ管の描出ができれば真のセンチネルリンパ節を確認することは容易である。さらに、われわれは、色素法、SPIOによる間質内MRリンパ造影、放射性コロイドSPECT/CTリンパシンチグラフィの3者の新しい比較試験を計画中である。

結論として、マウスを用いた比較試験で、頭頸部領域のセンチネルリンパ節描出能に関して、放射性コロイドSPECT/CTリンパシンチグラフィは間質内MRリンパ造影よりも優れた結果が得られた。しかし、頭頸部領域でSPIOもしくはferucarbotranを用いた間質内MRリンパ造影はSLNBに用いられる可能性が示された。

本研究は平成23年度厚生労働省科学研究費補助金（H21-がん臨床-一般-016）の援助を受けた。